MIT
International Center for
Air Transportation

Evaluation of the Impact of Transport Jet Aircraft Approach and Departure Speed on Community Noise

Prof. R. John Hansman
Jacqueline Thomas

Report No. ICAT-2020-03
April 2020

MIT International Center for Air Transportation (ICAT)
Department of Aeronautics & Astronautics
Massachusetts Institute of Technology
Cambridge, MA 02139 USA

Technical Report Documentation Page

1. Report No.	2. Government Accession No.	3. Recipient's Catalog No.
ICAT-2020-03_Thomas_Hansman		

4. Title and Subtitle	5. Report Date
Evaluation of the Impact of Transport Jet Aircraft Approach and Departure Speed on Community Noise	April 2020
	6. Performing Organization Code

7. Author(s)	8. Performing Organization Report No.
R. John Hansman and Jacqueline Thomas	

9. Performing Organization Name and Address	10. Work Unit No. (TRAIS)
Center of Excellence for: Alternative Jet Fuels and Environment Massachusetts Institute of Technology Department of Aeronautics & Astronautics Cambridge, MA 02139	11. Contract or Grant No. 13-C-AJFE-MIT-008

12. Sponsoring Agency Name and Address	13. Type of Report and Period Covered
Federal Aviation Administration Office of Environment and Energy	Technical Report
	14. Sponsoring Agency Code

15. Supplementary Notes

https://dspace.mit.edu/handle/1721.1/126037

16. Abstract

This report evaluates the impact of changing aircraft speed during approach and departure on community noise for transport category jet aircraft. This analysis is part of a broader study investigating the opportunities to modify approach and departure procedures to reduce community noise impact. This report also addresses a requirement in Section 179 of the FAA Reauthorization Act of 2018 (H.R. 302) to evaluate the relationship between jet aircraft approach and takeoff speeds and corresponding noise impacts on communities surrounding airports.

17. Key Words	18. Distribution Statement
ASCENT	

19. Security Classif. (of this report)	20. Security Classif. (of this page)	21. No. of Pages	22. Price
Unclassified	Unclassified		

I. Introduction

This report evaluates the impact of changing aircraft speed during approach and departure on community noise for transport category jet aircraft. This analysis is part of a broader study investigating the opportunities to modify approach and departure procedures to reduce community noise impact. This report also addresses a requirement in Section 179 of the FAA Reauthorization Act of 2018 (H.R. 302) to evaluate the relationship between jet aircraft approach and takeoff speeds and corresponding noise impacts on communities surrounding airports.

II. Impact of Speed on Aircraft Source Noise

The primary sources of noise from aircraft are engine and airframe noise, as shown in Fig. 1. Historically jet engine noise has been the dominant noise source, particularly during high power settings on takeoff. Modern engines have become significantly quieter [1] and airframe noise has become increasingly important during landing and for some reduced power settings. Aircraft speed impacts engine and airframe noise differently, as discussed briefly below.

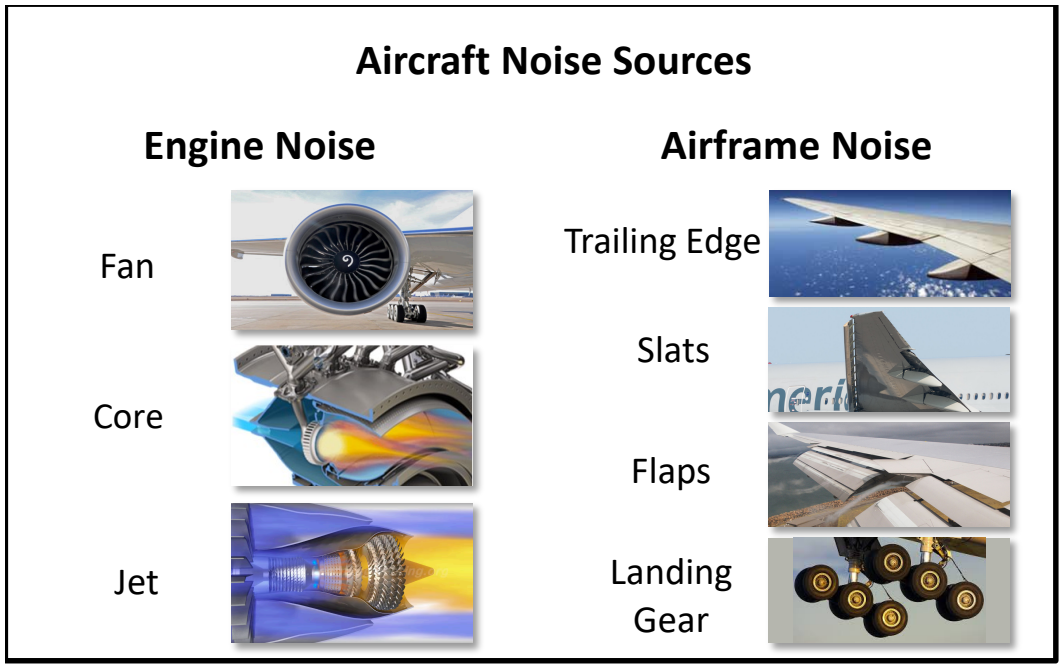

Fig. 1 Primary Conventional Turbofan Aircraft Noise Sources

Example breakdowns of the various noise components for a representative narrow-body jet transport aircraft after initial departure and on final approach are shown in Fig. 2. Engine noise is dominant on departure with most of the noise coming from the fan, followed by the jet. Airframe noise is more significant on approach, particularly due to the deployment of flaps, slats, and landing gear, and dominates the noise when engine settings are low. The exact magnitude

of noise components, and how they relate to each other, depends on the specific aircraft and flight procedure.

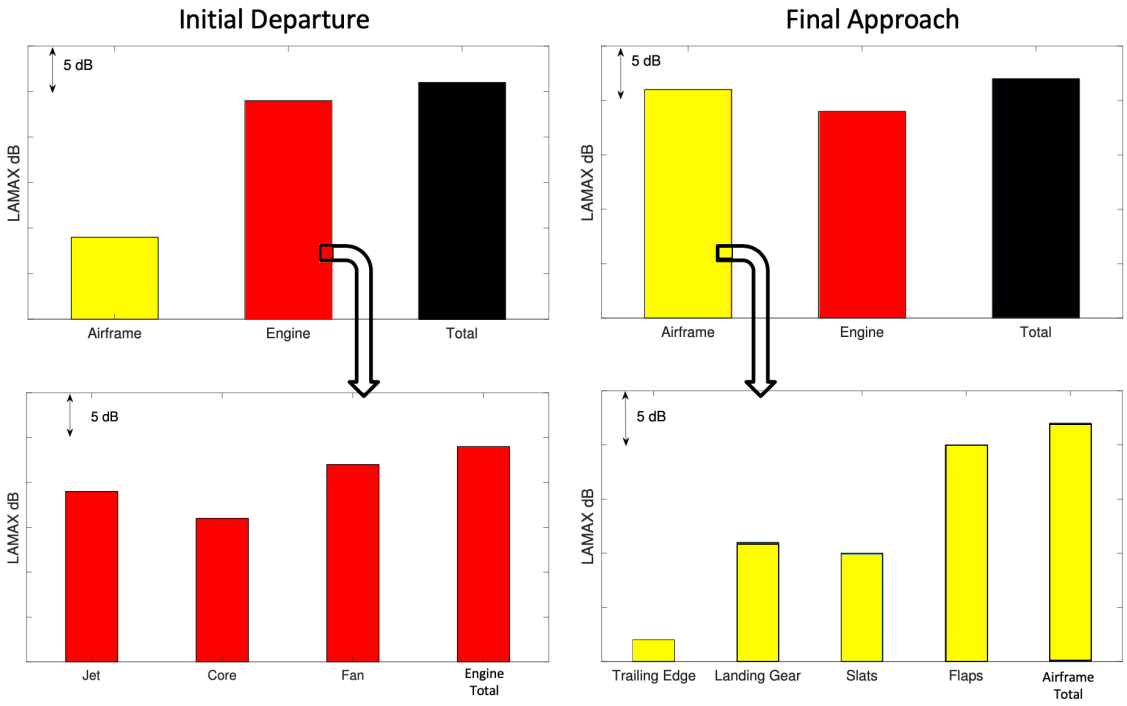

Fig. 2 Comparisons of Different Aircraft Noise Sources on Initial Departure and Final Approach for a Representative Narrow-Body Aircraft

1. Impact of Speed on Engine Noise

Engine noise arises primarily due to fan, combustion, and jet noise. *Fan* noise arises due to turbulent air passing rotating fan blades and stator vanes [2], *combustion* noise arises due to the combustion of hot gases in the engine core and subsequent propagation through the turbine [3], and *jet* noise arises primarily due to the turbulent mixing of fast jet exhaust airflow with slower ambient air [4]. In general, the engine noise will increase with increased power setting. Engine noise also increases with increasing difference between the speed of the high velocity jet airflow and the speed of the aircraft, which impacts the turbulent mixing of the shear layers in the engine exhaust.

2. Impact of Speed on Airframe Noise

Airframe noise comes from turbulence generated by the aircraft airframe, usually around geometry changes. This includes noise from the basic wing and tails, known as *trailing edge* noise, as well as additional noise from the devices that extend into the airflow such as *flaps*, *slats*, and *landing gear*. All of these airframe noise sources are highly sensitive to aircraft speed. Clean trailing edge and slat noise scales with velocity to the 5^{th} power [5][6]. Flap noise scales with the 5^{th} power of velocity for low frequencies and the 6^{th} power of velocity for high frequencies [7]. Landing gear noise scales with the 6^{th} power of velocity [8].

In addition to the source noise effect described above, speed is also tightly coupled to aircraft flight aerodynamics and therefore impacts the configuration of the aircraft (i.e. flaps, slats, and landing gear settings). At slower speeds, the flaps and slats are extended to reduce the stall speed, which causes an increase in airframe noise.

III. Modeling Framework

In order to model the effect of speed on community noise, a model that includes the effects of speed on each of the various aircraft noise components is needed. These detailed speed impacts on community noise are not captured in the Aviation Environmental Design Tool [9]. For this evaluation, the NASA Aircraft Noise Prediction Program (ANOPP) [10] was used as the base aircraft noise model. ANOPP is a semi-empirical model that computes noise from each of the sources discussed in section II, including engine sources (fan, core, and jet) and airframe sources (trailing edge, flaps, slats, and landing gear). In order to model these individual noise sources, ANOPP requires detailed inputs, including detailed aircraft geometries, internal engine performance states, and aircraft flight profile states (position, thrust, velocity, configuration). ANOPP outputs single-event noise grids which are then used for noise impact assessments. The modeling framework showing the source of these inputs is shown in Fig. 3.

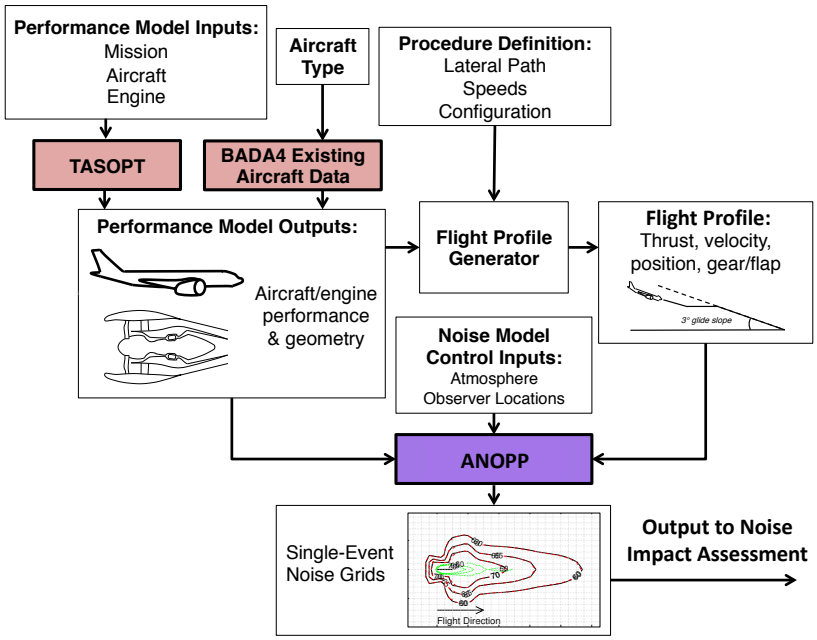

Fig. 3 Integrated Aircraft Performance, Flight Procedure, and Noise Analysis Process for Modeling Effects of Speed on Community Noise

Noise modeling requires the internal engine performance states, such as combustor exit temperature, as well as airframe geometry, including the wing, flap, slat, and landing gear geometry. Engine performance states that vary with the thrust and velocity throughout the approach or departure procedure are calculated using the Transport Aircraft System OPTimization (TASOPT) program [11], which is a physics-based model that jointly sizes and

optimizes the airframe, engine, and flight mission of a “tube and wing” transport aircraft. Engine sizing in this program is a work-balance-based, engine component matching formulation [12] that sizes an engine for design conditions and then provides engine state maps for off-design thrusts and flight speeds. The airframe geometry is also sized in this method based on aerodynamic and structural requirements and is verified from publicly available aircraft performance and geometry data for current aircraft [13][14]. With these inputs ANOPP provides component level aircraft noise estimates based on the thrust, velocity, configuration, position, and altitude changes in a flight profile. Use of these performance and noise tools has been validated against Federal Aviation Administration noise certification data [15].

The detailed flight profile (thrust, velocity, configuration, and altitude) of the approach or departure procedure of interest is computed by the Flight Profile Generator shown in Fig. 3. Based on a given arrival or departure procedure definition, such as a continuous descent or low thrust takeoff, the Flight Profile Generator computes the vertical flight profile—or the required thrust, velocity, and glideslope—with a point mass model that satisfies the weight, drag performance, and configuration speed limitations of a given aircraft. These flight performance characteristics are provided by Eurocontrol's Base of Aircraft Data (BADA 4) [16], a database of aircraft performance parameters from aircraft manufacturers and validated by comparison with ASDE-X radar observed flight profiles for current procedures.

For each arrival or departure procedure, the thrust, velocity, configuration, and altitude profiles are modeled on a segment-by-segment basis. Using the flight performance characteristics from BADA 4, force-balance is used to determine either: the flight path angle given a thrust and velocity or acceleration constraint, the resulting acceleration or velocity from a flight path angle and thrust constraint, or the resulting thrust from a flight path angle and velocity or acceleration constraint. This force balance process determines the acceleration/deceleration lengths, which are then integrated into the segment model to generate altitude, velocity, and thrust profiles versus flight path length.

Noise outputs are obtained as singe-event noise grids. Maximum A-weighted sound pressure level ($L_{A,MAX}$) is the primary noise metric at observer locations used in this paper. Outputted grids can be overlaid at desired airports and runways where the noise impact is to be measured. Population distributions from the 2010 census were used to measure population exposure to noise levels due to a specific flight procedure.

For each arrival and departure procedure evaluated in this report, the community noise impact was modeled for a representative narrow-body jet transport aircraft (Boeing 737-800 with CFM56-7B engines) and a representative wide-body jet transport aircraft (Boeing 777-300 with Trent 892 engines)).

IV. Effect of Aircraft Speed on Departure

1. Options to Change Aircraft Speed on Departure

In a typical departure procedure, shown in Fig. 4, the aircraft accelerates on the runway and performs its initial climb segment at a predetermined takeoff thrust and at an initial takeoff speed. The initial takeoff speed is dependent on aircraft takeoff weight and climb performance and set by safety considerations to provide a speed margin above the stall speed. Because of the criticality of stall margin and climb gradient at low altitude, the initial takeoff speed is not considered a candidate speed to be modified.

After reaching a transition altitude, usually between 1,000 ft and 2,000 ft, the thrust is reduced to a climb setting and the aircraft accelerates to a target climb speed. The thrust reduction is recommended for noise reduction in ICAO document 8168 [17]. The target climb speed is typically 250 knots, which is the maximum speed permitted below 10,000 ft in the United States. After the thrust reduction and as the aircraft accelerates, the flaps are incrementally retracted until the wing is in its flap and slat retracted configuration. This is consistent with what ICAO describes as Noise Abatement Departure Procedure 2 (NADP 2) in document 8168 [17].

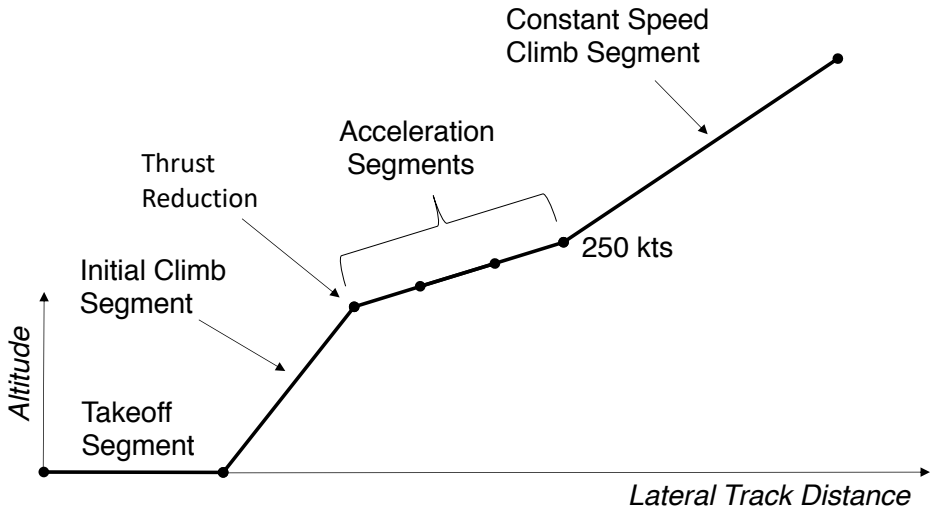

Fig. 4 Typical Departure Procedure Divided into Segments, Consistent with NADP 2.

There are two primary options to consider for varying speed in the departure phase after the takeoff and initial climb segment:

- Changing location of the start of acceleration and flap retraction
- Reducing the climb speed

2. Changing Location of the Start of Acceleration and Flap Retraction

Modifying the acceleration and flap retraction location has been considered previously. ICAO has recommended two procedures that consider where the location of the start of acceleration and flap retraction occurs in ICAO document 8168, published in 2006 [17]. They are Noise Abatement Departure Procedures (NADP) 1 and 2, shown in Fig. 5. These procedures are

used as examples to show how modifying the location of the start of acceleration and flap retraction impacts community noise.

In the NADP 1 procedure, after the initial thrust reduction at a cutback altitude, typically between 800 ft and 1,500 ft, the aircraft holds its initial climb speed of up to V2 + 20 knots[1] to an altitude of 3,000 ft. At 3,000 ft, the aircraft accelerates to its final climb speed of 250 knots. In the NADP 2 procedure, after the transition altitude, the aircraft accelerates to either its flaps up speed + 20 knots or its final climb speed.

The altitude gain of the NADP 1 between the thrust cutback altitude and 3,000 ft due to holding the slower speed of V2 + 20 knots is meant to benefit close in communities, while the altitude gain in the NADP 2 after the aircraft has accelerated to its final climb speed is meant to benefit far out communities. The NADP 2 is the standard procedure in the United States and NADP 1 is the standard procedure internationally.

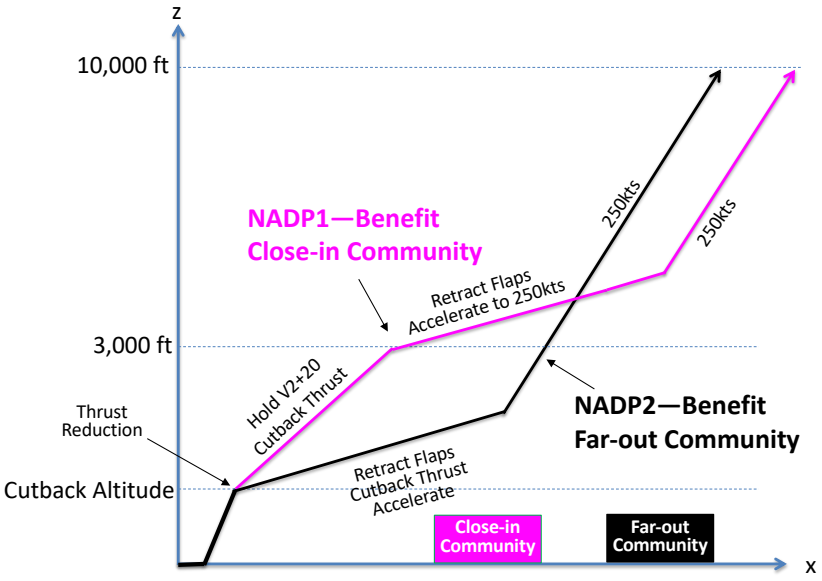

Fig. 5 Difference in Acceleration Height on Departure Represented by NADP 1 (3,000 ft Acceleration Height) and NADP 2 (1,500 ft Acceleration Height) Comparison.

The noise impact of a representative narrow-body jet aircraft (Boeing 737-800) performing an NADP 2 procedure compared to an NADP 1 procedure was investigated. The NADP 1 and 2 definitions do not specify the climb angle during the acceleration segments. Therefore, reference climb angles and velocities were determined to be the mean Airport Surface Detection Equipment, Model-X (ASDE-X) radar data observed at Boston Logan Airport (BOS) in 2017. An example of the observed altitude and velocity profiles from this data for Boeing 737-800 aircraft are shown in Fig. 6 along with the mean profiles. The velocity data shows that the start of

[1] V2 is the takeoff safety speed, or 1.2 times the stall speed on takeoff

acceleration occurs beginning after the initial cutback at about 1,500 ft, which is consistent with the NADP 2 procedure definition.

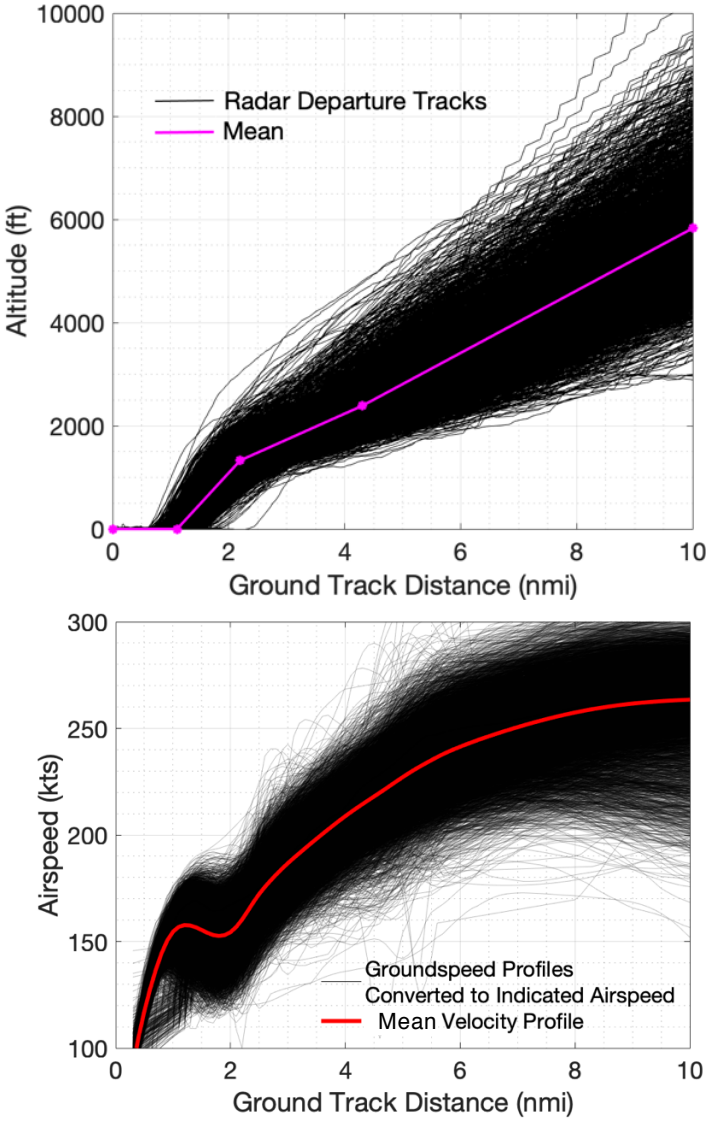

Fig. 6 ASDE-X Radar Altitude and Velocity Data of Boeing 737-800s on Departure at BOS in 2017.

Modeled flight profiles of the representative narrow-body aircraft for both the NADP 1 and NADP 2 are depicted in Fig. 7, which shows the comparison of altitude, velocity, and thrust profiles. The weight was assumed to be 90% of the maximum takeoff weight for this aircraft[2]. The thrust was assumed to be the same between the two procedures to provide a comparison of impacts due only to the change in acceleration height. Between the thrust cutback altitude and 3,000 ft, the aircraft performing the NADP 1 had a steeper climb angle than in the NADP 2 due to maintaining the slower V2 + 20 knots in this region rather than accelerating.

[2] Maximum Takeoff Weight assumed to be 174,000 lbs for the Boeing 737-800.

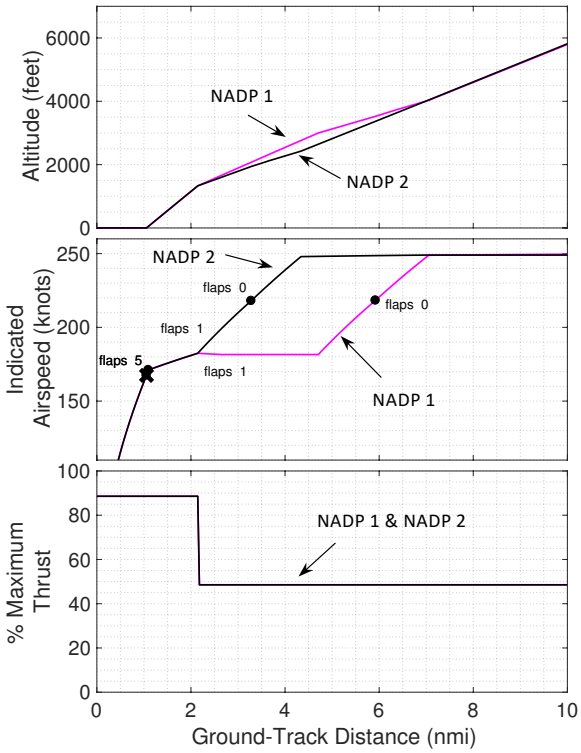

Fig. 7 Comparison of Altitude, Velocity, and Thrust Profiles for a Narrow-Body Aircraft Performing NADP 1 (magenta) and NADP 2 (black)

Noise impacts for the representative narrow-body aircraft performing the NADP 1 and NADP 2 are shown in Fig. 8, which presents the peak noise ($L_{A,MAX}$) under the flight track during a straight out departure. The difference in $L_{A,MAX}$ noise under the flight track for the NADP 2 and NADP 1 procedures is shown Fig. 9. Fig. 10 shows the corresponding $L_{A,MAX}$ contours.

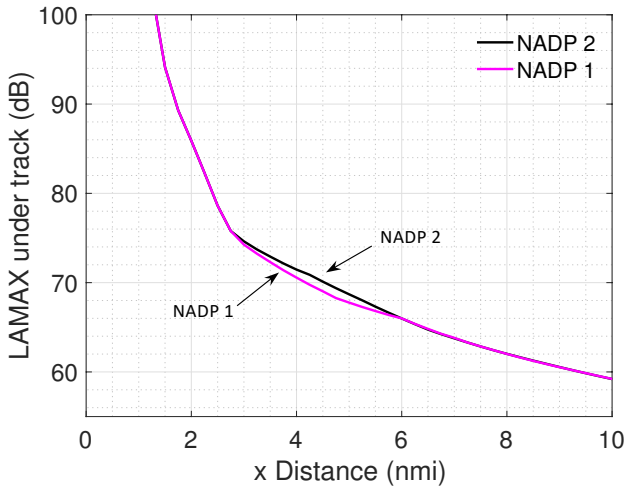

Fig. 8 Undertrack $L_{A,MAX}$ (dBA), NADP 2 and NADP 1 Noise for a Representative Narrow-Body Aircraft.

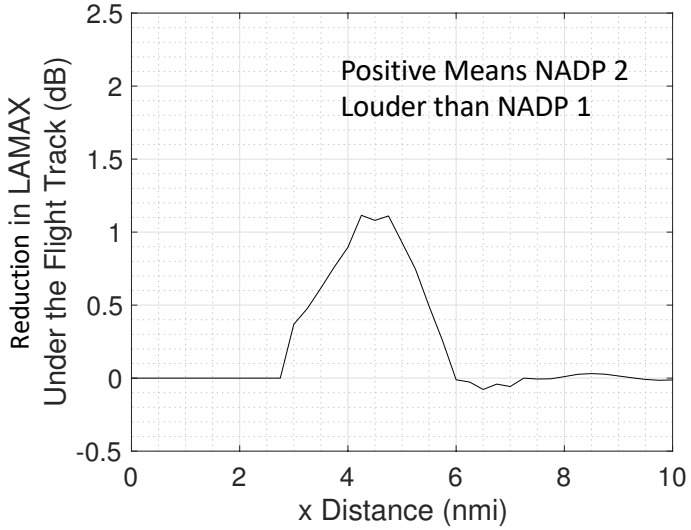

Fig. 9 Reduction in Undertrack $L_{A,MAX}$ (dBA), NADP 1 compared to NADP 2 for a Representative Narrow-Body Aircraft

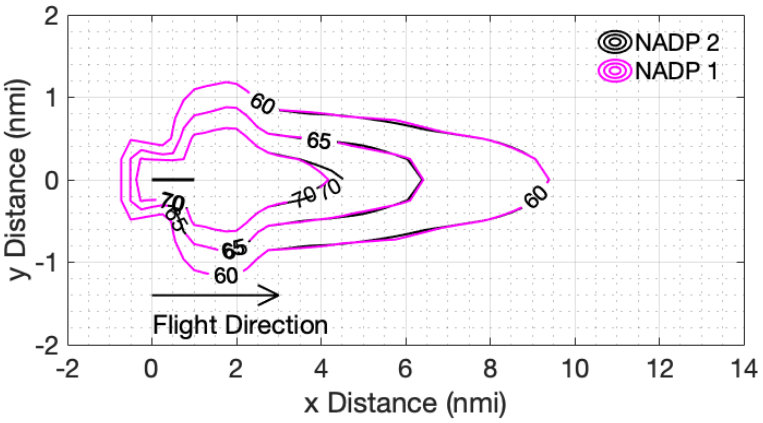

Fig. 10 NADP 1 and 2 $L_{A,MAX}$ (dBA) contours for a Representative Narrow-Body Aircraft

Fig. 9 shows NADP 1 results in a maximum noise reduction of 1.2 dBA between 3 and 6 nautical miles (nmi) from takeoff compared to the NADP 2 due to the extra altitude gained during the climb in this segment. This results in a small reduction of the extent of the 70 dBA LMAX contour when flying the NADP 1 compared to the NADP 2, as can be seen in Fig. 10. After 6 nmi the two procedures converge and there is insignificant difference between NADP 1 and NADP 2. The small, 1.2 dBA, maximum noise reduction occurs over a limited spatial area and is therefore not considered a significant noise reduction.

The NADP 2 procedure compared to an NADP 1 procedure was also investigated for a representative wide-body aircraft (Boeing 777-300) using a similar analysis. The reference altitude and velocity climb profiles for Boeing 777-300 departures at Boston Logan Airport (BOS) from 2017 are shown in Fig. 11. The velocity data shows that for Boeing 777-300 departures at BOS, the start of acceleration begins after the initial cutback at about 1,900 ft, which is also consistent with the NADP 2 procedure.

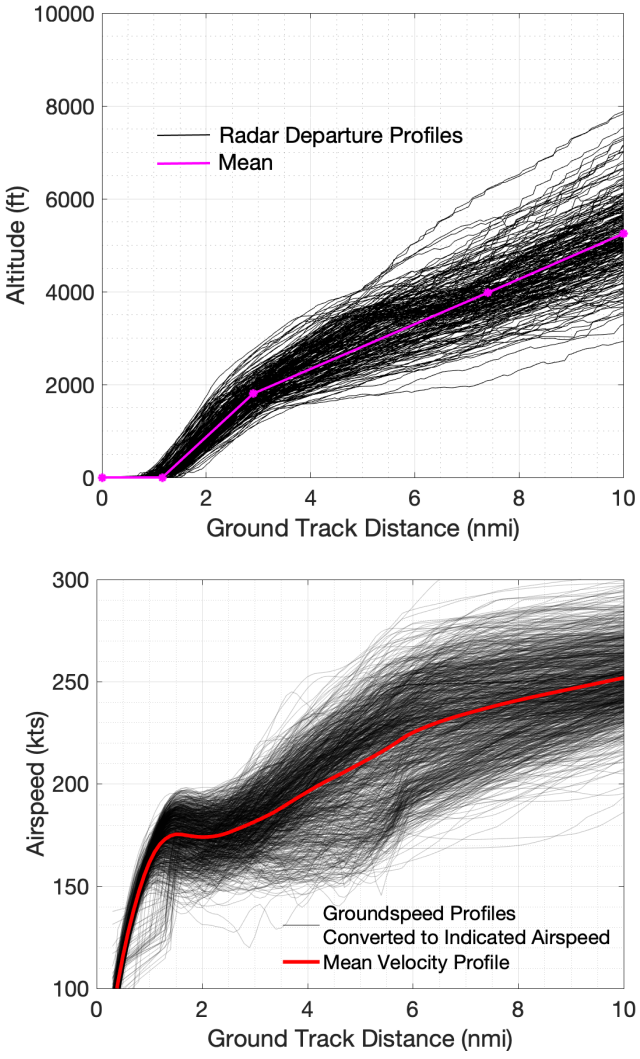

Fig. 11 ASDE-X Radar Altitude and Velocity Data of Boeing 777-300s on Departure at BOS in 2017.

Modeled flight profiles of the representative wide-body aircraft for both the NADP 1 and NADP 2 are depicted in Fig. 12, which shows the comparison of altitude, velocity, and thrust profiles. The weight was assumed to be 90% of the maximum takeoff weight for this aircraft[3].

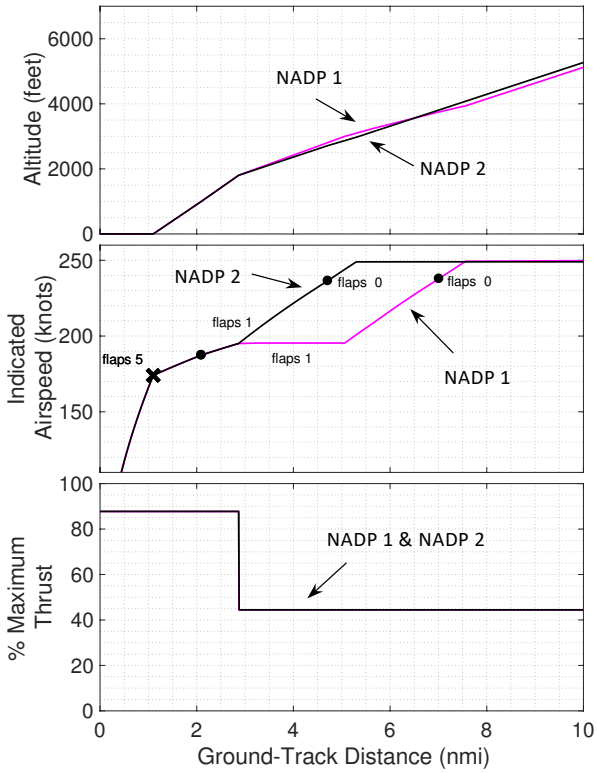

Fig. 12 Comparison of Altitude, Velocity, and Thrust Profiles for a Representative Wide-Body Aircraft Performing NADP 1 (magenta) and NADP 2 (black)

Noise impacts for the representative wide-body aircraft performing the NADP 1 and NADP 2 are shown in Fig. 13 as the peak noise ($L_{A,MAX}$) under the flight track during a straight out departure. The difference in $L_{A,MAX}$ is shown in Fig. 14. Fig. 15 shows the corresponding $L_{A,MAX}$ noise contours.

[3] Maximum Takeoff Weight assumed to be 659,550 lbs for the Boeing 777-300

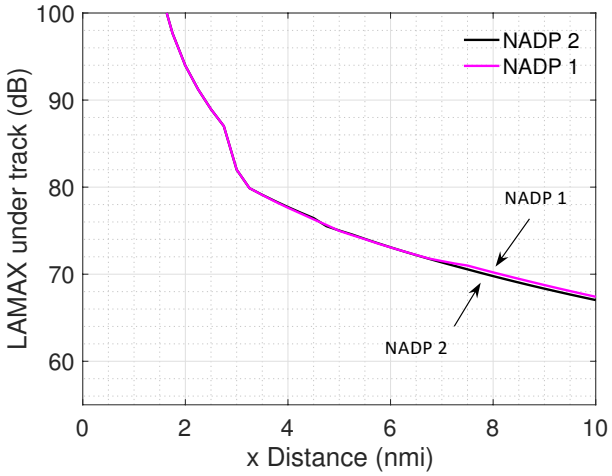

Fig. 13 Undertrack $L_{A,MAX}$ (dBA), NADP 2 and NADP 1 Noise for a Representative Wide-Body Aircraft.

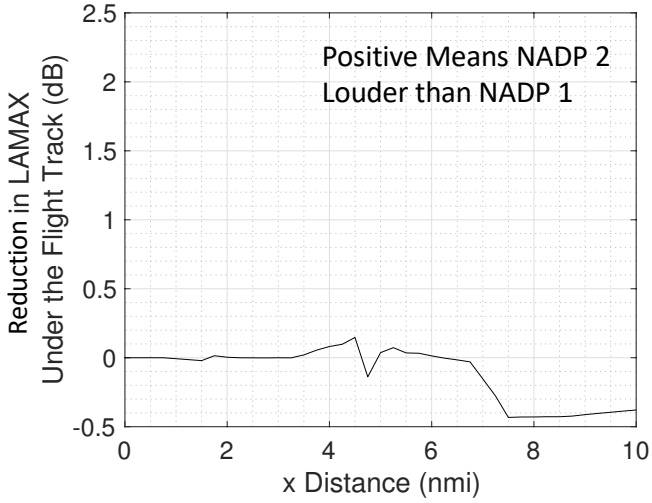

Fig. 14 Reduction in Undertrack $L_{A,MAX}$ (dBA), NADP 1 compared to NADP 2 for a Representative Wide-Body Aircraft.

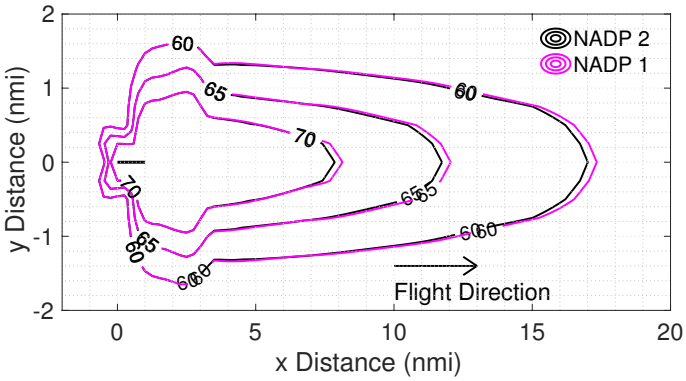

Fig. 15 NADP 1 and 2 $L_{A,MAX}$ (dBA) contours for a Representative Wide-Body Aircraft.

Fig. 14 shows that the undertrack noise levels are quite similar up until 7 miles after which the NADP 2 has a slightly lower (0.4 dBA) noise level due to the slightly higher altitude of the NADP 2 procedure in this region. This can also be seen in a small reduction of the 60, 65, and 70 dBA contours in Fig. 15.

The results show that changes in the acceleration location on departure results in small differences in community noise impacts compared to current departure procedures. Currently observed procedures in the U.S. are consistent with NADP 2 and it does not appear that changing the acceleration location would result in significant reduction in community noise impacts.

3. Reduced Climb Speed

Another option for varying the speed on departure is to reduce the climb speed after initial acceleration, which would reduce the airframe noise during the climb segment and would reduce the total noise if the airframe noise is greater than the engine noise. The typical departure from Fig. 4 was used to provide a basis of comparison to consider where varying the speed on departure would impact community noise.

In the reduced speed departures, aircraft were assumed to maintain the same weight, altitude profile, and velocity profile as the typical departure through the initial climb segment until the aircraft accelerated to the minimum safe airspeed with flaps up, which was maintained to 10,000 ft as shown in Fig. 16. The minimum safe airspeed in the flaps up configuration was assumed to be 1.3 x V_{stall}. The flaps up configuration was assumed to minimize flap noise and any icing impact during the climb. Aircraft were assumed to have maintained the same thrust profile as the typical departure, which results in higher climb profiles for the reduced speed departures. A speed of 220 knots was assumed to be the minimum safe airspeed in the flaps up configuration for the representative narrow-body aircraft, while 240 knots was assumed for the representative wide-body aircraft. The weight was assumed to be 90% of the maximum takeoff weight for both aircraft as referenced in the previous section.

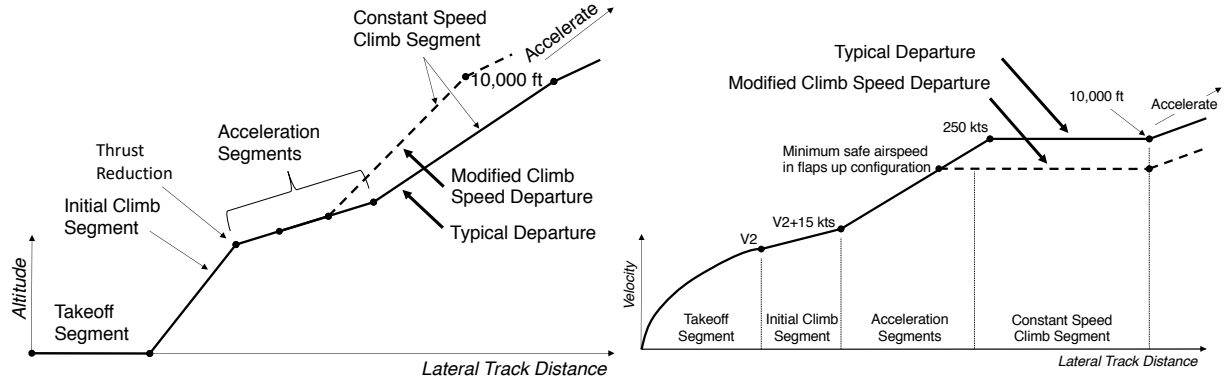

a) altitude profile b) velocity profile

Fig. 16 Reduced Climb Speed Departure Definitions.

Because the flaps, slats, and gear are retracted during a reduced speed climb, the airframe noise is from only the trailing edge noise and thus improvement from a reduced climb speed would only occur only if the trailing edge noise is greater than the engine noise during climb. The trailing edge noise is normally not measured during standard certification flight testing which is focused on measuring noise in the landing or takeoff conditions when the flaps, slats and landing gear are extended. As a consequence there is very little public data for trailing edge noise for modern aircraft in the clean (flaps, slats and gear retracted) configuration.

The ANOPP noise model for trailing edge noise uses a correlation generated from flight tests conducted by NASA in the 1970s [18][19] of multiple aircraft in flaps up, gear up, idle thrust[4] configurations, at flight speeds up to 350 knots. This data was used to formulate the trailing edge noise model by Fink used in ANOPP [5]. The original 1970s data is shown in Fig. 17. The noise magnitude was found to be a function of the 5^{th} power of the flight velocity. The flight test data also showed a residual variability for different aircraft types which was suggested to be due to variability in wing surface aerodynamic smoothness between high performance sailplanes and conventional aircraft. Fink observed an 8 dBA difference in the correlation lines used for conventional wing surfaces of the 1970s and aerodynamically smooth wing surfaces as shown by the solid lines in Fig. 17. The ANOPP noise model has the option to use the "aerodynamically smooth" or "conventional" wing surface assumption. Based on the public 1970s data, most transport aircraft would have the louder "conventional" wing surface.

Recent data provided by NASA [20] and Boeing for modern aircraft and also plotted on Fig. 17 indicate that modern aircraft wing technologies have a lower clean trailing edge noise level closer to the "aerodynamically smooth" aircraft assumption. As a consequence, the quieter "aerodynamically smooth" trailing edge noise levels were used in this analysis.

[4] While taking measurements with engines off would have been ideal for measuring clean airframe noise, large aircraft such as the Convair 990 and the Boeing 747 were instead tested at idle thrust to mitigate safety risks [17].

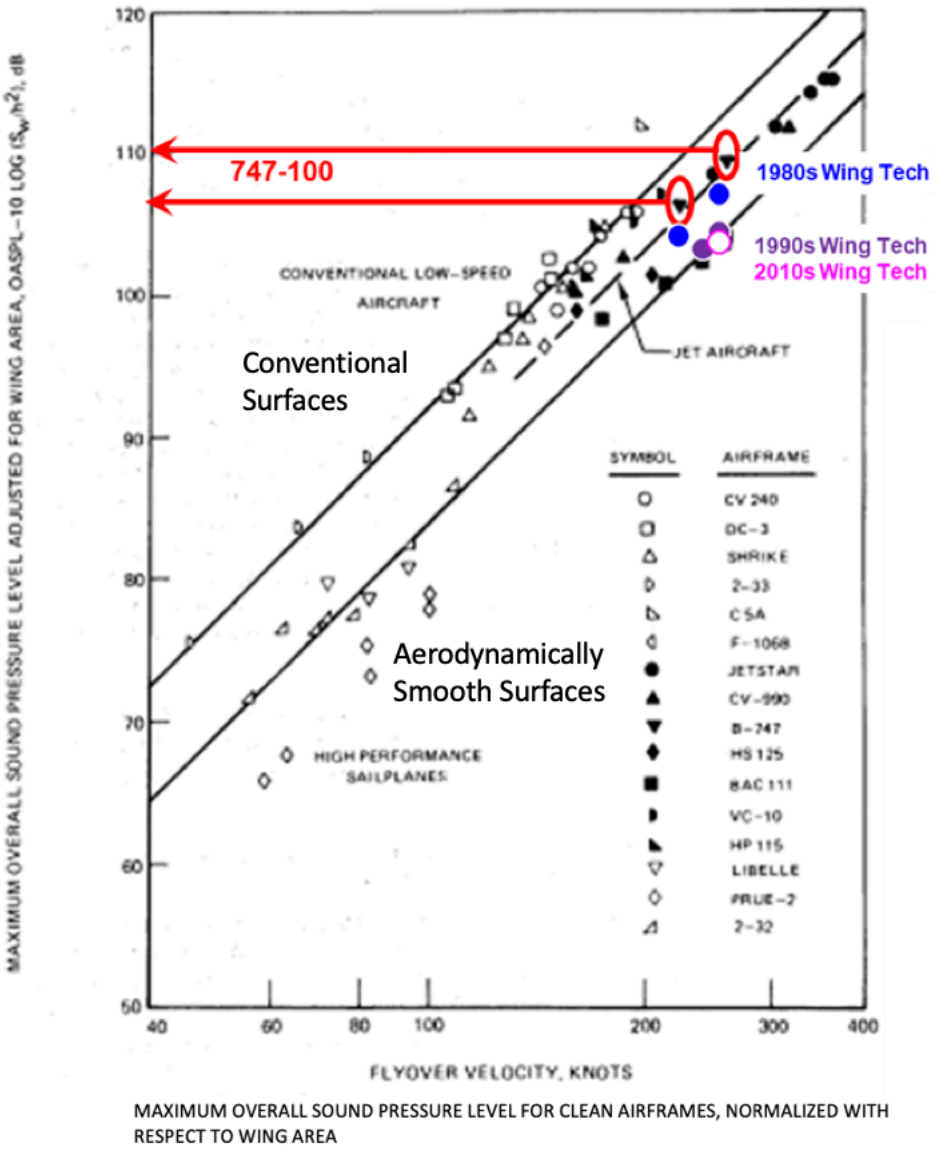

MAXIMUM OVERALL SOUND PRESSURE LEVEL FOR CLEAN AIRFRAMES, NORMALIZED WITH RESPECT TO WING AREA

Fig. 17 Maximum Overall Sound Pressure Level From 1970s flight Fight Tests of Aircraft with Flaps and Gear Up versus Velocity from Ref. [5]. 1980s, 1990s, and 2010s Wing Tech Data Provided by Boeing from Ref. [21]

The noise impacts of the representative narrow-body aircraft performing reduced speed departures compared to typical departures was investigated. The $L_{A,MAX}$ noise under the flight track for the 220 and 250 knots climb speeds are shown in Fig. 18. The corresponding difference in $L_{A,MAX}$ noise under the flight track between the 250 knots climb speed departure and 220 knots climb speed departure is shown in Fig. 19. The reduction in noise from reducing the climb speed from 250 to 220 knots occurs between 3.5 and 8 miles and is less than 0.5 dBA.

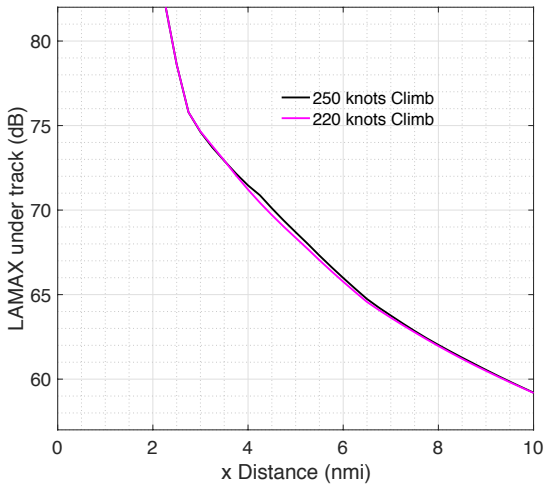

Fig. 18 $L_{A,MAX}$ (dBA) Under the Flight Track for 250 knot Climb Speed Departures and 220 knot Climb Speed Departures for a Representative Narrow-Body Aircraft.

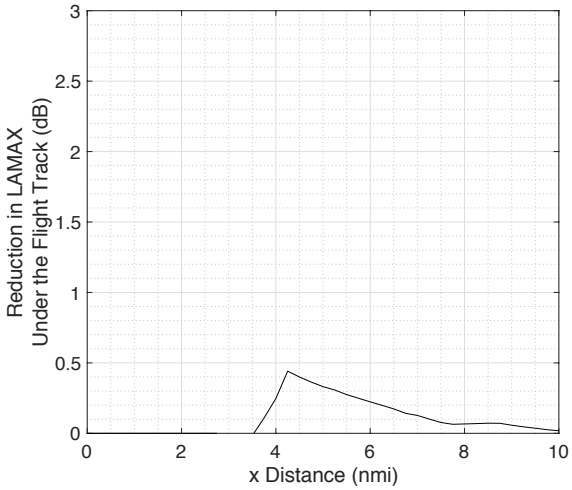

Fig. 19 Reduction in $L_{A,MAX}$ (dBA) for 220 knot Compared to 250 knot Climb Speed Departure for a Representative Narrow-Body Aircraft.

Engine, airframe, and total $L_{A,MAX}$ noise contours of a takeoff for the representative narrow-body aircraft are shown in Fig. 20 for typical and reduced climb speeds of 250 knots and 220 knots with the aerodynamically smooth wing surface assumption.

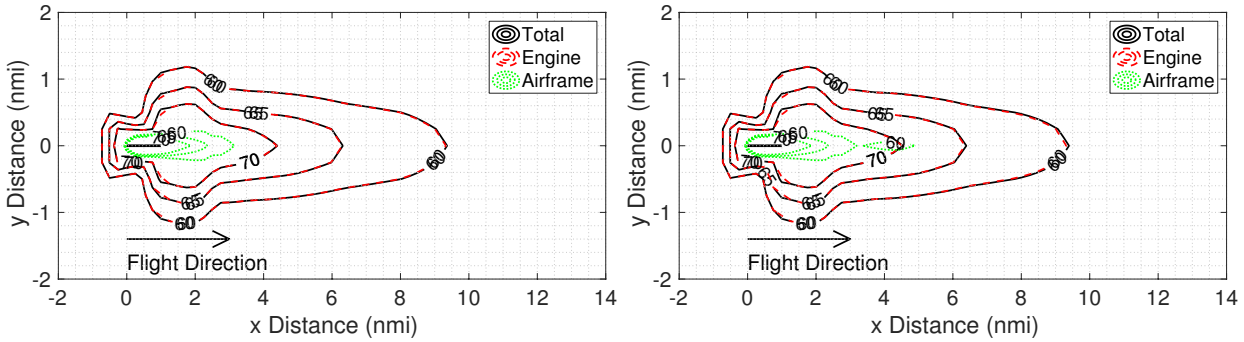

a) 220 knots climb speed b) 250 knots climb speed

Aerodynamically Smooth Wing Surface Assumption

Fig. 20 $L_{A,MAX}$ (dBA) Noise Contours 220 and 250 knot Climb Speed Departures for a Representative Narrow-Body Aircraft.

The reason for there being only a small noise difference from varying the climb speed can be seen in the noise contours in Fig. 20, which break out the airframe and engine noise. Because the noise is dominated by engine noise during the climb the climb speed does not have a significant effect on the noise contour.

Similar trends in noise impact were seen for the representative wide-body aircraft. The $L_{A,MAX}$ noise under the flight track for the 240 and 250 knot climb speeds with the "aerodynamically smooth" wing surface assumption is shown in Fig. 21. The difference in the resulting $L_{A,MAX}$ noise under the flight track is insignificant as shown in Fig. 22. Again this is due to the dominance of engine noise during climb, which can be seen in the noise contours in Fig. 23.

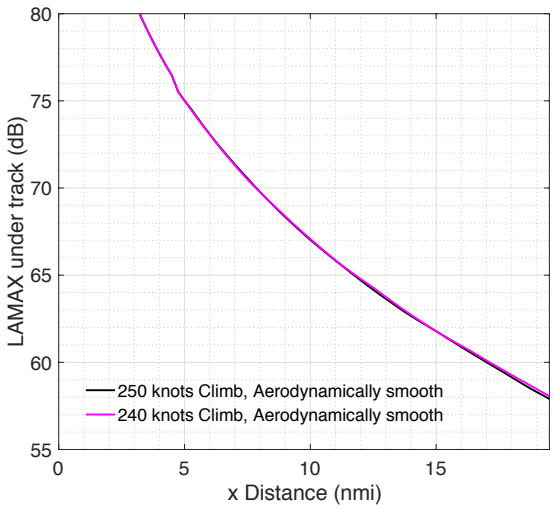

Fig. 21 $L_{A,MAX}$ (dBA) Under the Flight Track for 250 knot Climb Speed Departures and 240 knot Climb Speed Departures for a Representative Wide-Body Aircraft.

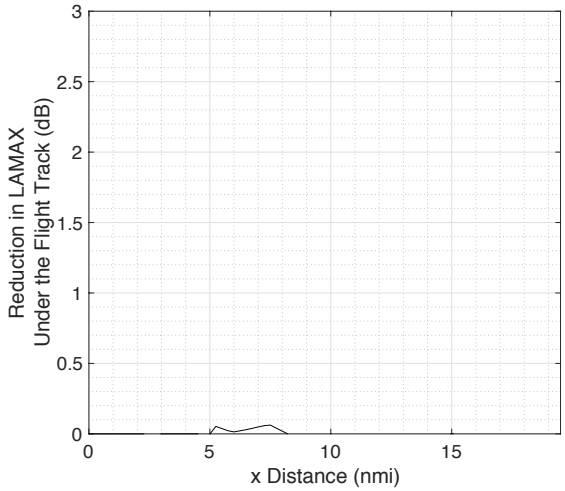

Fig. 22 Reduction in $L_{A,MAX}$ (dBA) for 220 knot Compared to 250 knot Climb Speed Departure for a Representative Wide-Body Aircraft.

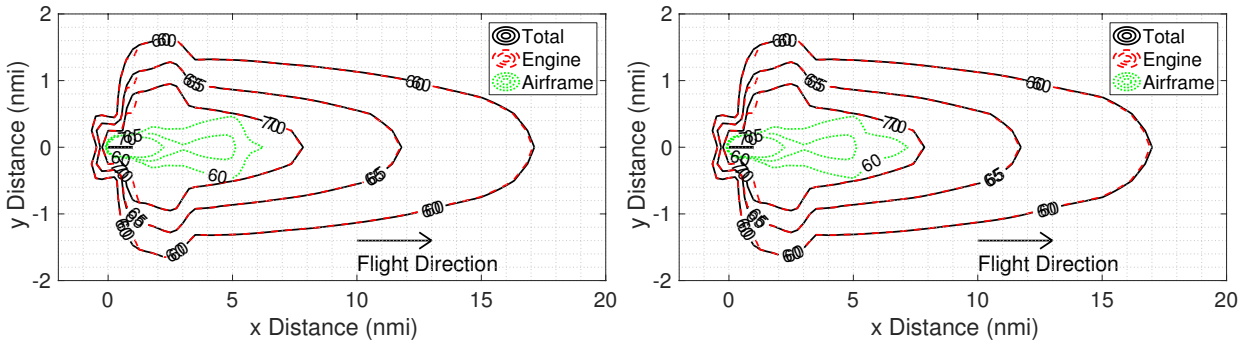

a) 240 knots climb speed b) 250 knots climb speed

Aerodynamically Smooth Wing Surface Assumption

Fig. 23 $L_{A,MAX}$ (dBA) Noise Contours 240 and 250 knot Climb Speed Departures for a Representative Wide-Body Aircraft.

V. Effect of Speed on Approach

1. Options to Change Aircraft Speed on Approach

A typical approach procedure is shown in Fig. 24 to provide a basis of comparison to consider where varying the speed on approach would impact community noise. Typical approach procedures consist of an initial descent segment from a starting altitude, deceleration segments where flaps and slats are deployed, a level segment and an interception with the Instrument Landing System (ILS) glide slope (in some cases the approach procedure may also be a continuous descent to the ground), and a final descent to touchdown, as depicted in Fig. 24.

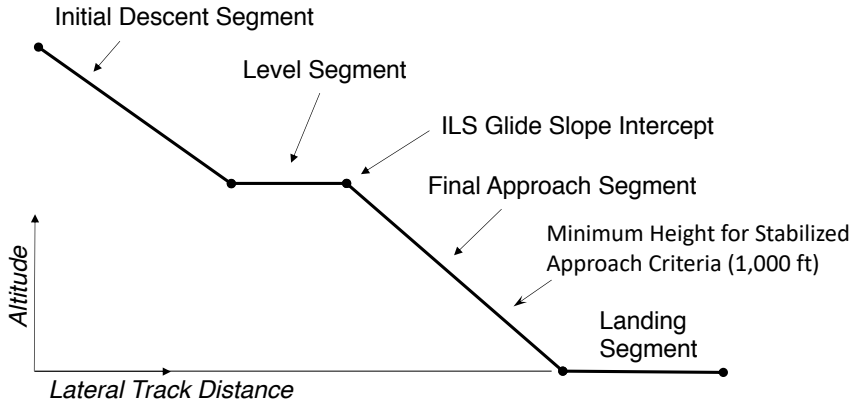

Fig. 24 Typical Approach Procedure Divided Into Segments

The Flight Safety Foundation Approach-and-Landing Accident Reduction Briefing Note 7-1 suggests that all aircraft should meet the stabilized approach criteria at a minimum of 1,000 feet above the airport surface in instrument meteorological conditions [22], meaning the aircraft is fully configured for landing and at a constant final approach speed between V_{REF} and V_{REF} + 20 knots[5]. This point is highlighted on Fig. 24. The stabilization point may occur further from touchdown than 1,000 ft.

Example approach procedures from Airport Surface Detection Equipment, Model X (ASDE-X) radar for Boeing 737-800 approaches into Runway 4R at Boston Logan International Airport (BOS) in 2017 are depicted in Fig. 25. The data show aircraft typically leveling off at 4,000 ft before intercepting the ILS glide slope. The 4000 ft level segment is consistent with published ILS procedure for Runway 4R at BOS, however the presence and altitude of published level segments vary due to ATC and terrain considerations. Fig. 25 also shows the corresponding velocity profiles which show most of the flights are stabilized in speed at 1,700 ft, corresponding to the outer marker location at BOS runway 4R [23]. Before the stabilization point, deceleration locations and rates vary, as is seen in the velocity data in Fig. 25. The mean velocity profile is

[5] V_{REF} is the landing reference speed, or 1.3 times the stall speed with landing flaps and depends on the weight and density altitude

shown in red. An example of a velocity trajectory for an aircraft which decelerated early is shown in green while an example of an aircraft which delayed its deceleration is shown in blue.

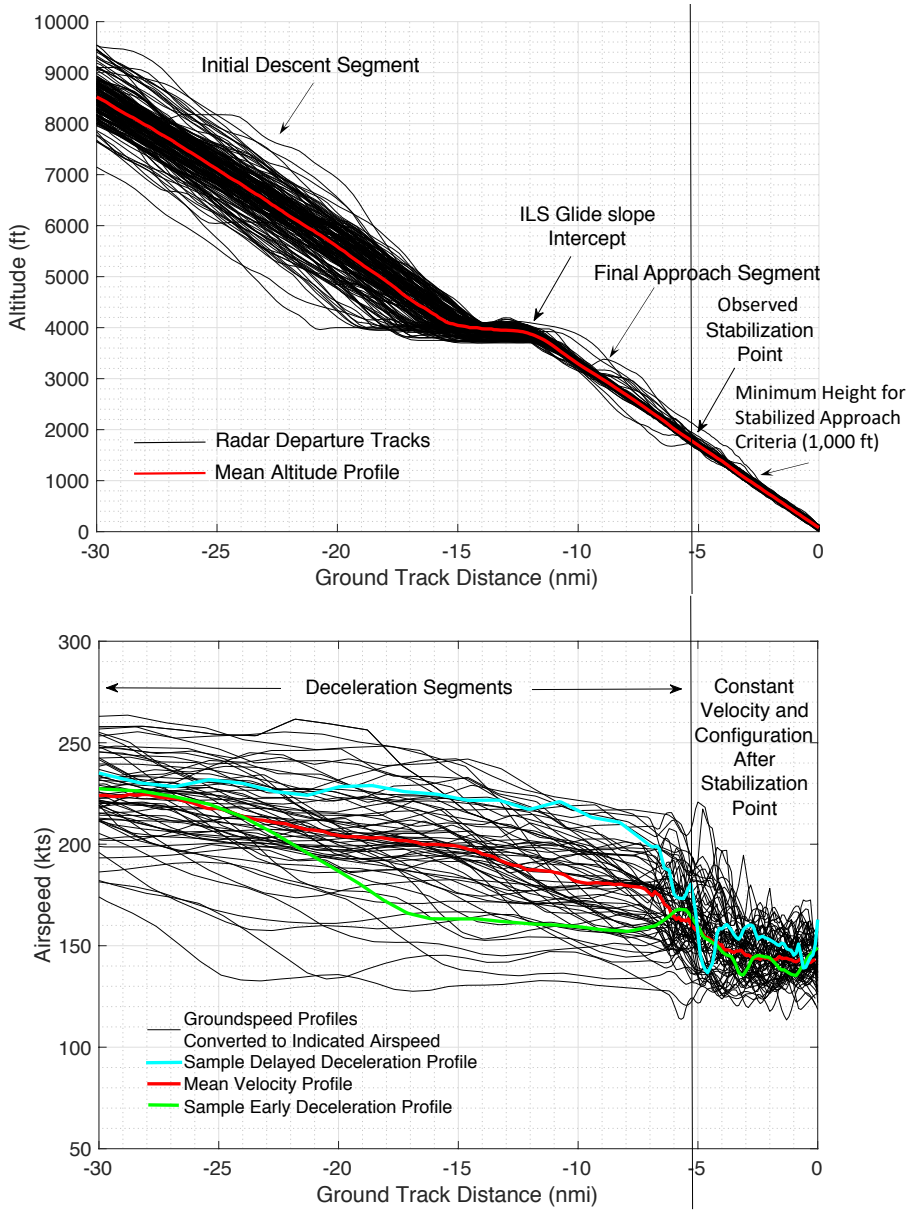

Fig. 25 ASDE-X Radar Altitude and Velocity Data of Boeing 737-800s Performing ILS Approaches with 4,000 ft Level-Offs into Runway 4R at BOS in 2017.

Flaps and slats are required to be deployed when speeds are reduced on approach to allow the wing to maintain lift at the lower speeds and to provide drag to slow the aircraft. Aircraft have multiple flap/slat configurations (typically 4 to 7) and deploy flaps and slats when they have decelerated to 10 knots below the maximum allowable speed for each configuration. Aircraft that decelerate relatively early in the approach require flaps and slats to be deployed early and to increase engine thrust to compensate for the additional drag for much of the

approach profile [24]. This results in an early onset of configuration noise from flaps and slats and additional engine noise for early deceleration approaches.

An alternative is a delayed deceleration approach. In a delayed deceleration approach, the deceleration is delayed such that the aircraft can have flaps and slats up and operate at low thrust for as long as possible to reduce both configuration and engine noise. The aircraft deceleration is delayed to a location such that it is still able to slow to the final approach speed prior to the stabilization point. Prior analyses have shown that the reduced flight time and thrust during this type of procedure yields significant reductions in fuel burn [24]. The reduced thrust and delaying of flap and slat deployment are also beneficial for noise.

2. Delayed Deceleration Approach

Varying speed on approach involves delaying the start of the deceleration segments, known as a delayed deceleration approach, while maintaining the safety requirement that the aircraft must be fully configured and at the final approach speed prior to the stabilization point. Speed, altitude, configuration, and thrust are highly coupled on approach and various combinations of approaches can be carried out. In this section, example noise impacts of a representative narrow-body and wide-body aircraft performing a delayed deceleration approach procedure are compared to a standard deceleration approach.

Flight profiles of the representative narrow-body aircraft (Boeing 737-800) for both baseline and delayed deceleration approach procedures were generated and are shown in Fig. 26. The weight was assumed to be maximum landing weight[6]. The baseline case is a 3 degree ILS approach with a 4,000 ft level-off and a standard deceleration profile. The standard deceleration profile was assumed to be the mean deceleration profile seen in the ASDE-X velocity data in Fig. 25. Flap and slat deployment were assumed to occur once the aircraft decelerated to 10 knots below the maximum slat and flap speeds for each configuration. The 1,700 ft location, which corresponds to the outer marker location at BOS runway 4R [23], was assumed to be the stabilization point where the aircraft was at the final approach speed, assumed to be V_{REF} + 10 knots—and fully configured for landing. This was consistent with observations and represents a 700 ft buffer from the stabilized approach criteria minimum height of 1,000 ft.

The baseline case is compared to a delayed deceleration approach. For the delayed deceleration approach, the location of the start of the deceleration from 250 knots was assumed to be the point at which at idle thrust, the aircraft would be able to meet the final flaps 30 configuration speed at 2,000 ft. The resulting flight profiles are shown in Fig. 26. The distance to touchdown where the flaps 1 through flaps 30 configuration settings were deployed are marked on the indicated airspeed profiles.

[6]The maximum landing weight for a Boeing 737-800 assumed to be 146,000 lbs.

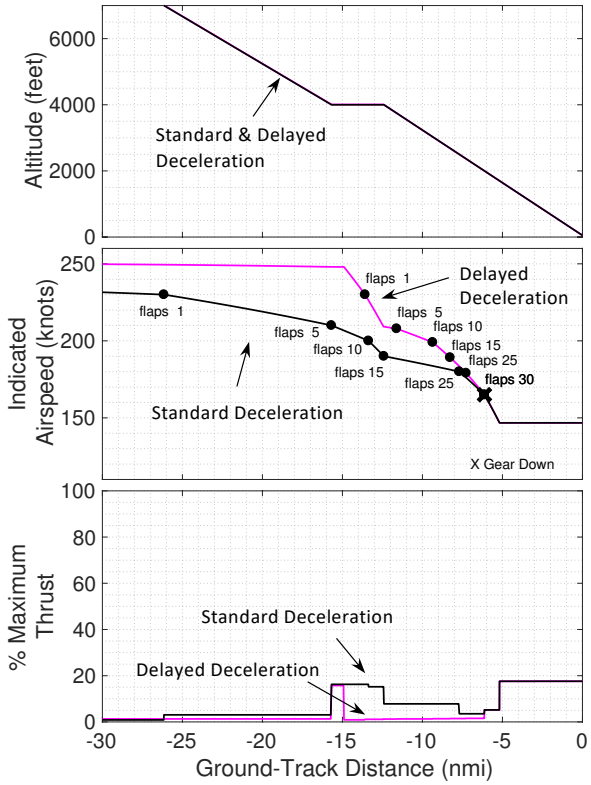

Fig. 26 Altitude, Velocity, and Thrust Profiles for a Representative Narrow-Body Aircraft Performing Standard Deceleration (black) and Delayed Deceleration (magenta) Approaches with 4,000 ft Level-Off

The black lines in Fig. 26 represent the velocity and thrust profiles of the baseline, standard deceleration approach and the magenta lines represent the profiles for the delayed deceleration approach. Once the aircraft decelerates the thrust must increase to maintain velocity in order to meet the stabilized final approach velocity which results in the higher thrust levels for the standard deceleration. The locations of flap deployment are closer to touchdown for the delayed deceleration approach, and the thrust is at idle for most of the procedure.

Fig. 27 shows the reduction in the total $L_{A,MAX}$ noise under the flight track due to the delayed deceleration approach compared to the standard deceleration. Modeled $L_{A,MAX}$ under the flight track of the various noise components for the ILS procedure with a 4,000 ft level-off is shown in Fig. 28 for reference.

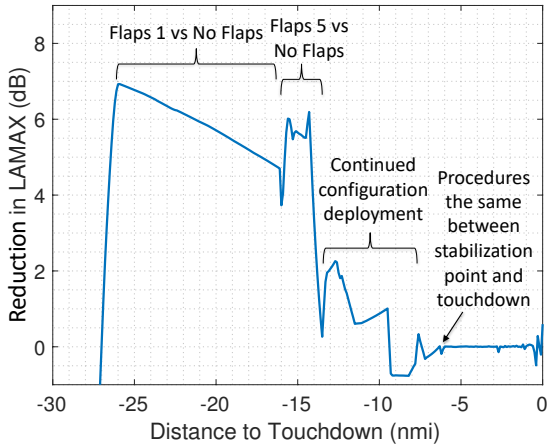

Fig. 27 Reduction in $L_{A,MAX}$ (dBA) Under the Flight Track for Delayed Deceleration Approach Compared to Standard Deceleration for a Representative Narrow-Body Aircraft,

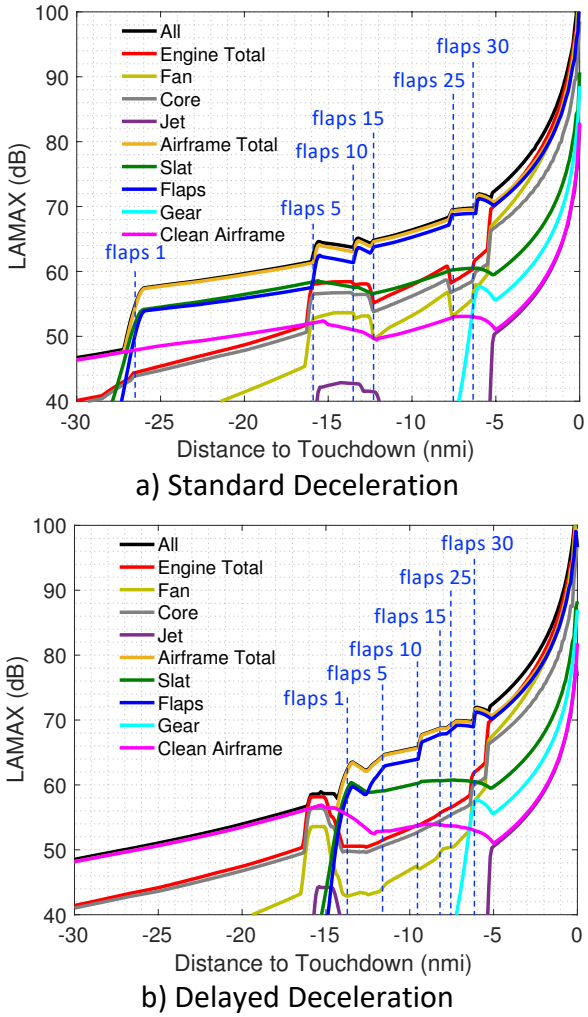

Fig. 28 Noise Levels Under the Flight Track for Different Noise Components, Representative Narrow-Body Aircraft Approaches with 4,000 ft Level-Off

As Fig. 27 indicates, between 26 and 16 nmi from touchdown, flaps 1 were deployed in the standard deceleration case but not in the delayed deceleration case. Noise is reduced by approximately 6 dBA by delaying the flaps 1 deployment in this region. Between 16 and 14 nmi from touchdown, flaps 5 were deployed in the standard deceleration case but no flaps were deployed in the delayed deceleration case, resulting in an additional 6 dBA reduction in this region. The most significant reductions are beyond 14 nmi from touchdown. No difference in the noise is observed between the stabilization point at 6 nmi and touchdown. Fig. 28 shows that the flap and slat noise dominate the overall noise levels before the stabilization point. The delay in the flap and slat deployment, as well as the decrease in thrust, resulted in a delay in the flap and slat noise onset and decrease in engine noise for the delayed deceleration approach compared to the standard deceleration approach. Thus, delaying the deceleration such that the aircraft can maintain the flaps and slats up configuration and idle thrust levels for as long as possible in the approach in this example would have a significant impact on reducing community noise.

Similar results were observed for a representative wide-body aircraft (Boeing 777-200). Noise impacts of the representative wide-body aircraft performing a delayed deceleration approach procedure are compared to a standard deceleration procedure below.

Flight profiles for both baseline and delayed deceleration approach procedures were generated and are shown in Fig. 29. The weight was assumed to be maximum landing weight[7]. The baseline case was a 3 degree ILS approach with a 4,000 ft level off with a standard deceleration profile. The standard deceleration profile was assumed to be the mean deceleration profile seen in the ASDE-X data for Boeing 777-200 aircraft at Boston Logan Airport in 2017. Flap and slat deployment were assumed to occur once the aircraft decelerated to 10 knots below the maximum slat and flap speeds for each configuration. The 1,700 ft location, which corresponded to the outer marker location at BOS runway 4R [23], was assumed to be the stabilization point where the aircraft were at V_{REF} + 10 knots and fully configured.

For the delayed deceleration approach, the location of the start of the deceleration from 250 knots was assumed to be the point at which at idle thrust, the aircraft would be able to meet the final approach configuration of flaps 30 speed at 2,000 ft. The resulting flight profiles are shown in Fig. 29. The distance to touchdown where flaps 1 through flaps 30 were deployed are marked on the indicated airspeed profiles.

[7] The maximum landing weight of the Boeing 777-200 assumed to be 455,000.

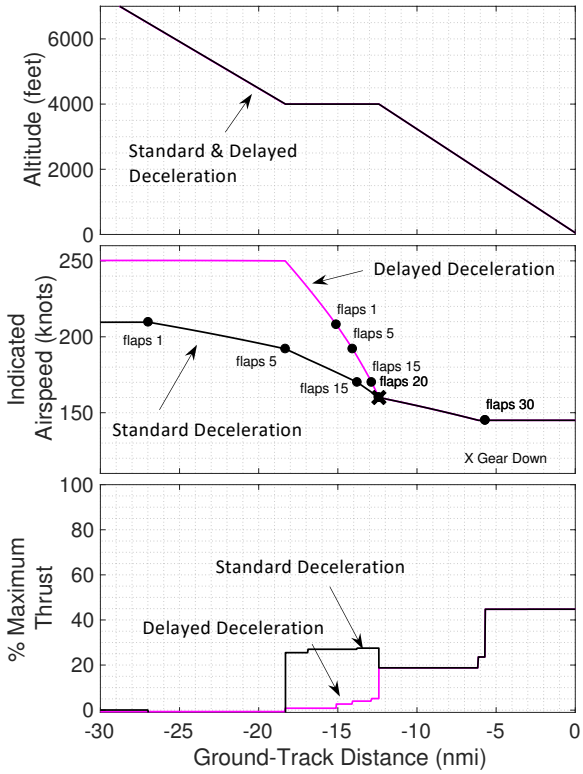

Fig. 29 Altitude, Velocity, and Thrust Profiles for Representative Wide-Body Aircraft Performing a Standard Deceleration (black) and Delayed Deceleration (magenta) Approach with 4,000 ft Level-Off

The black lines in Fig. 29 represent the velocity and thrust profiles of the baseline standard deceleration approach and the magenta lines represent the profiles for the delayed deceleration approach. Flaps 20 and gear down are required for this aircraft to have enough drag to perform the 3 degree final descent after the ILS intercept. Thus, the two procedures are the same after the ILS intercept.

Fig. 30 shows the reduction in the total $L_{A,MAX}$ noise under the flight track due to the delayed deceleration approach compared to the standard deceleration. Modeled $L_{A,MAX}$ under the flight track of the various noise components for the ILS procedure with a 4,000 ft level-off is shown in Fig. 31 for reference.

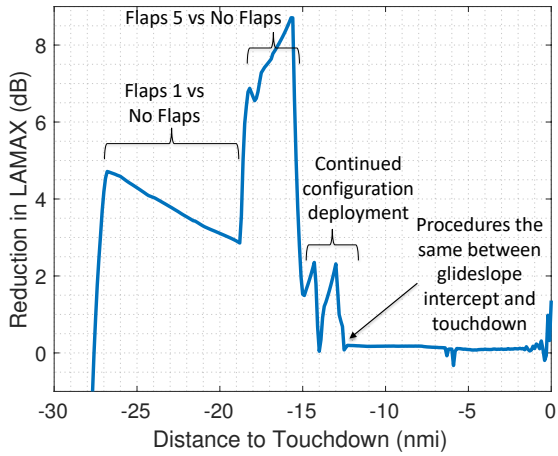

Fig. 30 Reduction in $L_{A,MAX}$ (dBA) Under the Flight Track for Delayed Deceleration Approach Compared to Standard Deceleration for Representative Wide-Body Aircraft

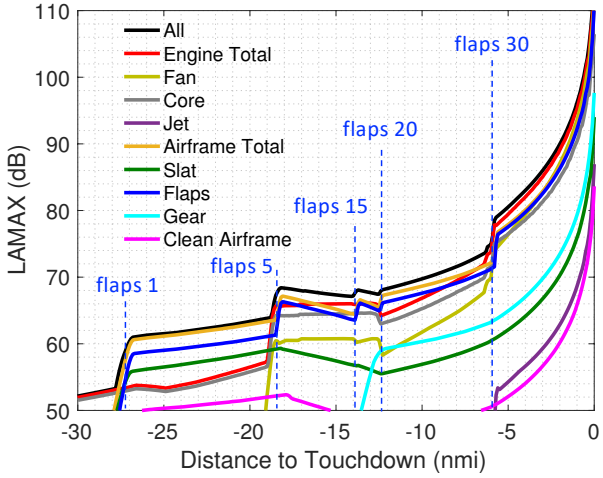

a) Standard Deceleration

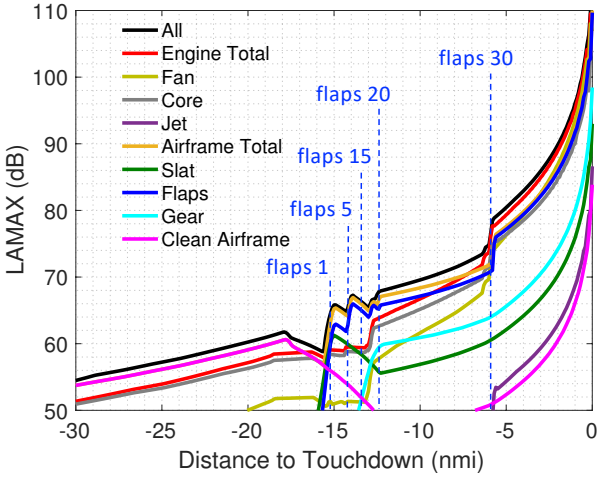

b) Delayed Deceleration

Fig. 31 Noise Levels Under the Flight Track for Different Noise Components, Representative Wide-Body Aircraft Approaches with 4,000 ft Level-Offs

As shown in Fig. 30, noise is reduced by about 4 to 8 dBA by delaying the deceleration and subsequent flaps 1 and flaps 5 deployment. The most significant reductions are beyond 15 nmi from touchdown. The delay in the flap and slat deployment, as well as the decrease in thrust during the level segment between 19 and 13 nmi to touchdown, results in a decrease in the configuration noise and engine noise for the delayed deceleration approach compared to the standard deceleration approach. After the intercept with the ILS at 13 nmi, the two procedures have the same noise impact. In this example, beyond the ILS intercept at 13 nmi from touchdown, delaying the deceleration such that the aircraft can maintain a clean configuration and idle thrust levels for as long as possible is shown to have a significant impact on reducing community noise.

Significant noise benefits were observed when delaying deceleration and subsequent flap and slat deployment for both aircraft assessed. There does appear to be a significant noise benefit from delayed deceleration approaches.

3. Operational Implications of Delayed Deceleration Approaches

While there appears to be a significant noise benefit from delayed deceleration approaches, there are operational challenges associated with this procedure from both a cockpit and air traffic control perspective that require further study. One key issue is that the deceleration performance will vary by aircraft type. Even for the same aircraft type, the deceleration performance will be affected by aircraft weight as well as winds and air density.

From the cockpit perspective, pilots will need procedures or guidance to manage aircraft deceleration on approach considering aircraft weight, winds, and air density to assure that the aircraft reaches the stable approach criteria prior to the stabilization point. The guidance or procedures could include speed, thrust and configuration targets. Some initial work has been done on cockpit displays for planning optimal flap, slat, and landing gear release locations based on operating conditions. One example system is the Low Noise Augmentation System (LNAS) by DLR Flight Systems [25], which includes an electronic flight bag function that shows the closest or latest location from the runway where flaps, slats, and gear can be deployed and still meet the stable approach at a target location. Another similar system is an Airbus Flight Management System mode on the A350 that gives deceleration and flap deployment guidance [26].

From an air traffic control perspective, different deceleration rates for different aircraft will also create challenges in sequencing aircraft. Airborne aircraft are subject to minimum separation requirements. In general, aircraft must be separated by 3 nautical miles horizontally and/or 1,000 ft. vertically. Detailed separation requirements are specified in FAA Joint Order 7110.65Y [27]. Air traffic controllers must provide a sufficient time or distance interval between approaching aircraft to ensure the required separation between leading and trailing aircraft. However, the delayed deceleration schedules that yield the greatest noise reduction will vary by aircraft. As a result, research is required to determine how to implement delayed deceleration procedures and if aircraft specific procedures are warranted or if less aggressive decelerations that all aircraft can fly provide sufficient noise benefit.

An additional air traffic consideration is that procedure design criteria may need to be adjusted to allow larger turn radii which would be required for higher speed turns.

VI. Conclusion

This analysis shows that for modern aircraft on departure, changes in aircraft climb speed have minimal impact on the overall aircraft departure noise (less than 0.5 dBA over the entire departure procedure). Varying flap retraction and acceleration location was shown to result in minimal differences in the departure profile and small differences in noise (less than 1.2 dBA over the entire departure procedure). The current practice, which is consistent with the ICAO NADP 2 departure procedure, appears to be close to the minimum noise impact modeled.

This analysis shows that for modern aircraft on arrival, changes in approach airspeed could have a noticeable impact (reductions of 4-8 dBA) on the overall aircraft noise at relatively large distances from touching down (between 10 and 25 nmi from the runway). Engine thrust on approach is often low and thus airframe noise components, such as flap and slat noise, are more easily heard on approach than on departure. If aircraft decelerate early in an approach, then flaps and slats must be released. The release of these devices results in a noticeable change in approach noise. Thus, a delayed deceleration approach where deceleration is delayed such that the aircraft can maintain a flaps and slats retracted configuration for as long as possible while also delaying the need to increase thrust on approach is beneficial in terms of noise reduction. This procedure has the potential to reduce community noise but has implementation challenges, including the ability of pilots to know where to begin the deceleration for different aircraft weights and weather conditions and how air traffic controllers will sequence aircraft with different deceleration rates. Additionally, though the noise modeling shows a potential benefit from this concept, it is desired to validate this benefit through noise measurement of actual aircraft operations. These challenges require further study and are being supported by the FAA through the ASCENT Center of Excellence.

References

[1] O. Zaporozhets, V. I. (Vadim I. Tokarev, and K. Attenborough, *Aircraft noise : assessment, prediction and control*. Spon Press, 2011.

[2] M. Heidmann, "Interim Prediction Method for Fan and Compressor Source Noise," 1979.

[3] J. J. Emmerling, S. B. Kazin, and R. K. Matta, "Core Engine Noise Control Program, Volume III, Supplement 1 - Prediction Methods," 1976.

[4] J. R. Stone and F. J. Montegani, "An improved prediction method for the noise generated in flight by circular jets," 1980.

[5] M. Fink, "Airframe Noise Prediction Method," 1977.

[6] Y. Guo, "Aircraft Slat Noise Modeling and Prediction," in *16th AIAA/CEAS Aeroacoustics Conference*, 2010.

[7] Y. Guo, "Aircraft Flap Side Edge Noise Modeling and Prediction," in *17th AIAA/CEAS Aeroacoustics Conference (32nd AIAA Aeroacoustics Conference)*, 2011.

[8] Y. Guo, "Empirical Prediction of Aircraft Landing Gear Noise," Long Beach, 2005.

[9] G. G. Fleming, "Aviation Environmental Design Tool (AEDT)," *22nd Annu. UC Symp. Aviat. Noise Air Qual.*, no. June, 2016.

[10] W. E. Zorumski, "Aircraft Noise Prediction Program (ANOPP) Theoretical Manual," Hampton, 1982.

[11] M. Drela, "Transport Aircraft System OPTimization, Technical Description," Cambridge, 2016.

[12] J. L. Kerrebrock, *Aircraft engines and gas turbines*. Cambridge: MIT Press, 1992.

[13] *IHS Jane's aero-engines*. Coulsdon: IHS, Jane's Information Group, 2013.

[14] F. Jane, *All the World's Aircraft*. Marston: London Sampson Law, 1912.

[15] Federal Aviation Administration, "Aircraft Noise Levels," 2012. [Online]. Available: https://www.faa.gov/about/office_org/headquarters_offices/apl/noise_emissions/aircraft_noise_levels/. [Accessed: 26-May-2017].

[16] A. Nuic, "USER MANUAL FOR THE BASE OF AIRCRAFT DATA (BADA) REVISION 3.12," 2013.

[17] International Civil Aviation Organization, "Document 8168 - Aircraft Operations," 2006.

[18] T. W. Putnam, P. L. Lasagna, and K. C. White, "Measurements and Analysis of Aircraft Airframe Noise," *Aeroacoustics STOL Noise; Airframe Airfoil Noise*, vol. 45, pp. 363–378, 1976.

[19] P. Fethney, "An Expirimental Study in Airframe Self-Noise," *Aeroacoustics STOL Noise; Airframe Airfoil Noise*, vol. 45, pp. 379–403, 1976.

[20] Y. Guo and R. Thomas, "On Aircraft Trailing Edge Noise," in *25th AIAA/CEAS Aeroacoustics Conference*, 2019.

[21] T. Christenson, G. Barker, and E. Nesbitt, "Commercial Aircraft Clean Wing Airframe Noise Levels – Comparison with NASA ANOPP Fink Model," The Boeing Company, Boeing Document ROI 19-00375BCA, 2019.

[22] Flight Safety Foundation, "Stabilized Approach FSF ALAR Briefing Note 7.1," Alexandria VA, 2009.

[23] "ILS OR LOC RWY 04R," 2018. [Online]. Available: https://skyvector.com/files/tpp/1803/pdf/00058IL4R.PDF%0D%0D%0A.

[24] T. Reynolds, M. Sandberg, J. Thomas, and R. J. Hansman, "Delayed Deceleration Approach Noise Assessment," in *16th AIAA Aviation Technology, Integration, and*

Operations Conference, 2016.
[25] M. Scholz and F. Abdelmoula, “Active Noise Abatement Using the Newly Developed Pilot Assistance System LNAS,” in *InterNoise 2017*, 2017.
[26] Airbus, “Control your Speed, During Descent, Approach and Landing,” *Safety First*, no. 24, 2017.
[27] Federal Aviation Administration, “FAA Order JO 7110.65Y: Air Traffic Control,” 2019.